PCCP

Simultaneous neutron diffraction and microwave dielectric characterisation of ammine materials – a non-destructive, non-contact method for determining ammonia structure in solids

Journal:	*Physical Chemistry Chemical Physics*
Manuscript ID	CP-ART-06-2016-004249.R1
Article Type:	Paper
Date Submitted by the Author:	25-Jul-2016
Complete List of Authors:	hartley, jon; University of Nottingham, Jones, Martin; University of Oxford, Inorganic Chemistry Laboratory Porch, Adrian; Cardiff University, School of Engineering

Simultaneous neutron diffraction and microwave dielectric characterisation of ammine materials – a non-destructive, non-contact characterisation tool for determining ammonia content in solids

Martin Owen Jones[1], Jon Hartley[1, 2] and Adrian Porch[2]

1. STFC Rutherford Appleton Laboratory, Harwell Oxford, Didcot, OX11 0QX
2. Cardiff School of Engineering, Cardiff University, Queen's Buildings, The Parade, PO Box 925, Cardiff, Wales, CF24 3AA

Abstract

We have investigated ammonia adsorption in group two halides (MgI_2 and $CaBr_2$) using custom-built apparatus that permits simultaneous neutron diffraction, microwave dielectric characterisation and out-gas mass spectroscopy of solid state materials during ammonia adsorption. Deuterated ammonia was flowed over the sample and the uptake – as measured by mass flow meters, mass spectroscopy and structure – compared with the change in dielectric constant. An excellent correlation between ammonia content and dielectric property was observed and, when linked to diffraction, mass flow and mass spectroscopy data, could be used to determine the amount of ammonia present within the solid. The combination of these techniques could also be used to differentiate physisorbed and metal-coordinated ammonia and explain subtleties in the observed structural transformations.

Introduction

Ammonia is one of the most abundantly produced inorganic chemicals, with some more than 120 M tonnes produced worldwide annually, and its numerous industrial and agricultural uses are well known.[1] Ammonia has been promoted as a potential vector to buffer sustainable energy harvesting, chemically store hydrogen, due to its high hydrogen content (17.8 wt%) and its ability to store 30% more energy per liquid volume than liquid hydrogen.[2,3] Other applications include refrigeration,[4] on-board Selective catalytic reduction,[5] and separation and storage of ammonia during synthesis.[6] More recently, ammonia has been promoted as a potential vector to buffer sustainable energy harvesting, chemically store hydrogen and provide an on-board answer to NOx emissions from diesel vehicles. If any of these applications are to be realised a safe and efficient method for ammonia storage must be developed. In 2006 Norskøv[5] proposed the use of solid state halides to reversible and safely store ammonia. These materials were shown to reversibly store ammonia at high gravimetric and volumetric densities, with low vapour pressures. Subsequently, Johnson *et al* showed that ammonia could be reversible stored at densities that approached liquid ammonia, with evolution temperatures of less than 100 ^{o}C.[7] A complete review of the history and potential technological applications of solid state ionic ammine materials can be found in reference.[8]

Ammonia is a highly polar molecule (of electric dipole moment 1.47 D, about 80% of that of water) and therefore the adsorption and desorption of ammonia into and from a solid material will give rise to a large change in a material's dielectric properties.[9] Thus, observation of changes in dielectric properties can give a direct measure of the amount of ammonia adsorbed within a solid and, potentially, evidence for the mechanisms of adsorption and desorption. The dielectric properties of solids may be accurately and precisely determined using microwave resonator cavities.[10,11] A Microwave cavity resonator (MCR) operates when a signal at a specific frequency creates a resonance inside the cavity. This resonance depends upon the internal dimensions of the MCR and the medium in which the microwave fields propagate through the cavity. When a material is placed

within the cavity space with a relative permittivity ε the propagating fields will be perturbed causing a change in the MCR frequency of resonance.[12] The change in resonant frequency, Δf_0, from its unloaded resonance, f_0, relates to the polarisation, ε_1, caused by the presence of the material within the cavity. The change in resonant bandwidth, Δf_B, (3 dB or half-power) relates to the dielectric losses, ε_2, in the material. The combination of these measurements gives the complex relative permittivity of a dielectric material as $\varepsilon = \varepsilon_1 - j\varepsilon_2$, where the relationship between complex permittivity of the sample and changes in resonance are shown in the approximate formulae derived from the perturbation equation (eqn (1) and (2).[13,14]

$$-\frac{\Delta f_0}{f_0} \approx \frac{(\varepsilon-1)V_s}{2V_{eff}} \quad (1)$$

$$\frac{\Delta f_B}{f_0} \approx \Delta\left(\frac{1}{Q}\right) \approx \frac{\varepsilon_2 V_s}{V_{eff}} \quad (2)$$

Where V_s is the sample volume, V_{eff} is the mode volume, i.e. the effective volume of electric field energy within the cavity and Q is the quality factor of the cavity defined as $Q = f_0/f_B$.

We have developed a novel microwave cavity resonator that can measure the dielectric properties of solids dynamically under ammonia flow and in conjunction with neutron diffraction and mass spectroscopy techniques. This combination of techniques allows us to directly investigate the changes in dielectric properties on ammonia adsorption, correlate these changes with structure and quantified ammonia adsorption and thus utilise dielectric properties as a measure of coordinated ammonia within the solid state. The highly penetrating nature of neutrons allows us to construct the MCR from a highly conducting metal, in this case aluminium, which interacts poorly with the incoming neutron beam and has a high microwave quality Q factor, giving us an excellent dielectric sensitivity. Fully deuterated ammonia (ND_3) is used as the coordinating species due to the high coherent scattering for neutrons by deuterium (6.67 fm). This gives an excellent diffraction contrast for the ammine material with respect to the rest of the sample environment and the uncoordinated precursor salt. Two ionic salt materials were investigated, MgI_2 and $CaBr_2$. These materials were chosen for their thermodynamics and phase transformations on ammonia adsorption. It is important that the salt system have a comparatively low adsorption enthalpy and expansion coefficient as significant sample expansion and heating could lead to a rupture of the sample containment tube, and MgI_2 and $CaBr_2$ fall within the tolerances of our equipment. The structures of the precursor and ammines of MgI_2 are well known and therefore, the material serves as an excellent model. While the phase transformations and corresponding structures of the ammines of $CaBr_2$ are unknown, they should be similar to those of the well-studied $Ca[NH_3]_nCl_2$ and should provide a number of clear structural transitions.

Experimental

Experiments were performed at the POLARIS time-of-flight neutron powder diffractometer (NPD) at the pulsed spallation source ISIS in the Rutherford Appleton Laboratory.[15,16] The experimental rig, shown in Fig. 1, is designed to fit within the vacuum chamber of the NPD. A gas flow is directed through a quartz tube to the powered samples, which are held in place in the middle of the MCR with a silica frit. The MCR is a cylindrical host cavity, machined from aluminium in three parts, with internal dimensions of height 65 mm and radius 46 mm. The cavity structure has 21 mm holes at the top and bottom for placement of a thin-walled, low-loss quartz tube (of outer diameter 12 mm). The MCR has microwave chokes at the hole positions to ensure that the electromagnetic field is

contained within the cavity space and so minimise any radiation losses, which would otherwise reduce its Q factor. Cavity excitation is provided by a pair of square-flanged SMA jack connectors (supplied by Farnell) at radial positions 3 cm from the axis. These have open circuit terminations, with an extended centre conductor providing capacitive coupling to the electric field. A 20 mm section of the MCR wall is milled down to a depth of 1 mm to allow reduced attenuation of the neutron beam and coherent scattering from aluminium cavity. Nylon bolts were also used in the construction of the cavity to reduce the coherent scattering from the cavity structure. The internal dimensions of the MCR were chosen for the resonance mode TM_{010} to have a frequency of approximately 2.5 GHz. The cavity aspect ratio (height/radius) is chosen to be small enough for the TM_{010} mode to be the dominant mode (i.e. for it to be well below the resonant frequency of the TE_{111} mode), but not too small to compromise the high *Q* factor or the axial uniformity of the electric field. The TM_{010} mode is chosen for dielectric property measurement of the samples owing to the high and uniform electric field near the cavity axis. The electric field in this mode is directed parallel to the axis, thus parallel to the axis and walls of the sample tube, resulting in only minor modifications of the local electric field by the presence of the quartz tube.

Gas is supplied to the experimental rig from a custom built gas panel, with gas flow regulated by a mass flow controller and the outgas quantified by a mass flow meter (Chell CCD100) before passing to a mass spectrometer (HPR-20 QIC R&D Plus from Hiden analytical), which was set to monitor deuterated ammonia (ND_3), hydrogen, deuterium, argon, nitrogen, oxygen and water. Experiments were conducted at room temperature and pressure, and a diagrammatic depiction of the experimental set-up is shown in Fig. 2.

The MCR is connected via radio frequency (RF) coaxial cables to a Fieldfox N9912A vector network analyser (VNA). The transmitted microwave power from the VNA $|S_{21}|^2$ is measured in the frequency domain and non-linear, least-squares curve fitting to a Lorentzian response is used to determine resonant frequencies and loaded quality factors (denoted as Q_L). Microwave data was collected every 6 seconds. The random errors from the microwave measurement were calculated at less than ±1% in low loss dielectric conditions and up ±5% as dielectric losses increase. Due to the exothermic reaction of ammonia with the test material, the aluminium material of the MCR's walls would be expected to expand causing a reduction in conductivity and increases in both frequency and bandwidth due to temperature increase, respectively. Using another resonant mode (TM_{210}) which is independent of changes in the sample, the maximum change in MCR temperature is calculated to be 1.2°C in the $CaBr_2$ experiment and 1.7°C in the MgI_2 experiment. This temperature change relates to a 0.2% error in the $CaBr_2$ experiment and 0.7% in the MgI_2 experiment.

Systematic errors come predominantly from volume uncertainty, arising from sample expansion on ammonia adsorption, which is measured at around ±3%. The experimental rig was orientated in the POLARIS diffractometer so that the gas outlet pipe did not interfere with the diffracted signal from the back-scattering and 90° detectors. The beam dimensions were set at 2 cm height and 1.5 cm width to encompass the entire thinned aluminium wall window from the MCR. The neutron beam dimensions were set to 2 cm height and 1.5 cm width to encompass the entire thinned aluminium wall window of the MCR and diffraction data collected every 130 seconds with all diffraction data analysed by profile Rietveld refinement using the Topas software package.[17]

$CaBr_2$ sample was obtained in powder form and MgI_2 in the form of beads. The samples were prepared in an inert environment and weighted to an accuracy of 0.01 g. The MCR, support rig and quartz tube apparatus were assembled and flushed with argon. Background neutron diffraction, mass spectroscopy and dielectric measurements were made of the empty sample environment under argon gas flow. Once this was complete, the quartz tube was then loaded with 1.5 g of MgI_2 (99.998%, Sigma-Aldrich)or $CaBr_2$ (99.5%, Alfa Aeser) salt by opening a cap on the top of the rig, the cap reconnected, the whole assembly flushed with argon once again and VNA, diffraction, mass spectroscopy and dielectric data collection started simultaneously. Once data collection was confirmed for all 3 characterisation techniques, argon gas flow was switched to deuterated ammonia using the 3-way valve. Sample quantities were fixed at 1.5 g due to the tension between the requirements for a high signal-to-noise ratios in dielectric measurements, where large sample volumes and/or high loss materials attenuate the resonant signal, and a strong neutron scattering, where large sample volume is preferred due to the weak interaction of the neutron with matter. Neutron diffraction data sets were captured every 2 minutes (the fastest possible rate) and thus the ammonia flow was set as low as possible at 5 cm^3/min to optimise the quality of diffraction data collected during phase transformation processes.

Results

A surface plot of diffraction data from POLARIS Bank 4 for the ammoniation of $CaBr_2$ is shown in Fig. 3. At the onset of the experiment the scattered intensity is mostly associated with the scattering from the aluminium resonator. Very little scattering is observed from the ~1.5 g sample of $CaBr_2$ within the sample environment. This is not unexpected given the low physical cross section of the $CaBr_2$ within the beam in its starting state. As the ammonia is added, strong Bragg peaks begin to appear (point A in Figure 3) as the uptake of ammonia causes a considerable increase in volume of the sample (~300%, from 196 $Å^3$ for $CaBr_2$ to 580 $Å^3$ for $Ca[NH_3]_2Br_2$) and thus considerably increases the volume of the sample within the beam. Furthermore, the total scattering from the sample also increases as ammonia (ND_3) is adsorbed as the strongly coherent scattering D (6.67 fm) and N (9.37 fm) atoms are included within the structure. As the structure of $Ca[NH_3]_nBr_2$ is unknown, the initial Bragg peaks were fitted using the Pawley method, and a good fit was obtained using the $Ca[NH_3]_2Cl_2$ structure (space group Abm2, lattice parameter of a = 6.0042 Å, b = 7.8254 Å and c= 12.3494 Å) proposed by Westman *et al*[18] *as* a starting model) with refined lattice parameters of a = 6.006(6) Å, b = 7.77(1) Å and c= 12.33(1) Å. After 2.2 h, a clear structural transition is observed (point B, Figure 3). Based on the work of Liu *et al*[19] it was expected that the higher ammonia containing phase would be $Ca[NH_3]_6Cl_2$ or $Ca[NH_3]_8Cl_2$. The Bragg peaks for this new phase were again fitted using the Pawley method and a starting cell based on the $Ca[NH_3]_8Cl_2$ structure (space group Pnma, lattice parameter of a = 12.1143 Å, b = 7.3076 Å and c= 15.0829 Å) proposed by Westman.[18] A good fit was obtained with refined lattice parameter of = 10.354(16) Å, b = 7.327(9) Å and c= 15.077(18) Å, strongly suggesting that the new phase is the octa-coordinated complex since the observed volume (1143(3) $Å^3$) is close to that reported for $Ca[NH_3]_8Cl_2$ (1335 $Å^3$). It is also interesting to note that while $Mg[NH_3]_6Cl_2$ is known, there has as yet been no observation of hexa-coordinated $CaCl_2$, although $Ca[NH_3]_4Cl_2$ has been postulated. Given the increased anion radius of the bromide, it is unlikely that a hexa-coordinated equivalent would be stable.[20]

A surface plot of diffraction data from Bank 4 for the ammoniation of MgI_2 is shown in Fig. 4. At the onset of the experiment there is very little scattered intensity and that present may be associated with the scattering from the aluminium resonator. Very little scattering is observed from the 1.5 g sample of MgI_2 within the sample environment. As before, this is not unexpected given the low physical cross section of the MgI_2 within the beam in its starting state. As above, on addition of ammonia to the sample area (point A in Fig. 4), the sample begins to swell and strong Bragg peaks begin to appear. The uptake of ammonia causes a considerable increase in volume of the sample (~290%, from 118 $Å^3$ for MgI_2 to 340 $Å^3$ for $Mg[NH_3]_2I_2$ and thus considerably increases the cross-section of the sample within the beam.[3] The total scattering from the sample also increases as ammonia (ND_3) is adsorbed as the strongly scattering D (6.67 fm) and N (9.37 fm) atoms are included within the structure. $Mg[NH_3]_nI_2$ is known in two forms, n=2 [3] and n=6.[20] The Bragg data in Fig. 4 was fitted on the basis of both n=2 and n=6 phases, which appeared simultaneously on application of ND_3. Refined lattice parameters of a = 6.330(3) Å, b = 12.54(3) Å and c= 4.310(7) for the orthorhombic n= 2 phase and a = 10.985(3) Å for the cubic n= 6 phase were obtained, respectively. These are in good agreement with those published previously.[3,20] No structural transitions are observed for this material throughout the duration of the experiment as both phases are formed from the onset of ammonia dosing, although close inspection of the Bragg peak intensities for the n=2 and n=6 phases shows an increase in the n=6 phase as a function of exposure time.

A significant change in bandwidth and frequency as ammonia is adsorbed was observed. This behaviour was consistent with the inclusion of a polar molecule within the solid-state host.[21] As ammonia was adsorbed, the presence of the ammonia molecule both coordinated within the solid and physisorbed to the surfaces adsorbed the microwave energy within the sample, leading to an increase of bandwidth. This is a well-established feature of dielectrically lossy materials.[22] The corresponding increasing resonance-frequency shift to lower frequency again was consistent with the presence of a polar molecule which acts to increase the overall polarisation of the system. A plot of Bragg peak intensity (d = 3.17 Å) versus frequency shift (MHz) and change in Bandwidth for ammonia adsorption of MgI_2 is shown in Fig. 5. The dramatic change in dielectric properties was observed to commence with the increase in Bragg peak intensity and this change continued to increase until 4.2 h when the frequency and bandwidth ceased to increase and the Bragg peak intensity tended towards an asymptote. The change in Bragg peak intensity and polarisation suggested a first order adsorption dynamic (with the rate on change determined by the gas flow rate) of ammonia into the solid which was consistent with similar hydration studies.[23] The out gas contribution from the mass spectrometry supported this conclusion, as shown in Fig. 6. As ammonia was flowed through the system, argon was displaced and nitrogen/oxygen was observed in the out gas mass spectroscopy data. The presence of nitrogen and oxygen was due to ammonia adsorption by the material, resulting in a reduced gas flow to the mass spectrometer which then aspirates air to maintain sampling pressure.

From the frequency shift data the amount of ammonia adsorbed can be inferred assuming the linear change in frequency between 0.6 to 4.2 h is from the inclusion of ammonia into the host material. This is shown in eqn (3), where the slope is the linear fit of the region where ammonia is being adsorbed. The flow rate is in m^3/hr, f_{max} is the maximum change in frequency observed by the sample and the molar volume V_m at standard temperature and pressure. Using eqn (3) the total ammonia adsorbed in the 1.5 g sample of MgI_2 at 4.2 h was 0.0482 moles. By extension, knowing the

number of moles of ammonia adsorbed into the material mol, the mass of sample m and the molar mass of the sample M, these can then be used to calculate the amount of ammonia per unit formula in the material $(NH_3)_x$, as shown in eqn (4), which corresponds to 8.94 ammonia per unit formula.

$$mol = \frac{flow\ rate \times |\Delta f_{max}|}{slope \times V_m} \quad (3)$$

$$(NH_3)_x = \frac{mol \times M}{m} \quad (4)$$

At 7.2 h the ammonia flow into the system was replaced with argon and the resonance frequency was observed to increase by 1 MHz, suggesting a decrease in the overall sample polarization. A corresponding decrease in bandwidth of 270 kHz was also observed. These changes in dielectric properties were consistent with the loss of ammonia from the systems. Excess ammonia was also observed in the mass spectroscopy data from 7.2 h, which is consistent with the loss of ammonia from the system. It is thought that this shift of resonance to higher frequency and decrease in dielectric loss were due to the removal of physisorbed ammonia from the sample, as there is no noticeable change in the scattering intensity from the ammine phases in Fig. 4, as would be expected if coordinated ammonia were being removed. The bandwidth change (79.4%) was much more pronounced than that the frequency change (7.7%) (4.9% contributed by physisorbed ammonia 2.8% contributed by gaseous ammonia in the measurement space). Because the dielectric losses are highly influenced by the strength of dipolar bonds and the related rotational freedom of the ammonia molecule[24,25] we can infer that the physisorbed ammonia has stronger dipolar bonds than the coordinated ammonia. This causes more dielectric loss when the rotation of the ammonia molecule breaks the dipolar bonds of the physisorbed ammonia and thus a greater contribution to bandwidth shift. The degree of physisorbed ammonia may therefore be calculated using eqn (3), and a total of 0.0035 moles of physisorbed and gaseous ammonia was observed on flowing argon through the system. Taking this into account, the stoichiometry of our MgI_2 ammine becomes $Mg[NH_3]_{8.25}I_2$

For $CaBr_2$, it can be seen that there is a significant increase in bandwidth and frequency shift as ammonia is adsorbed (Fig. 7) and that this behaviour was consistent with the inclusion of a polar molecule within the solid-state host. The frequency shift apparent on ammonia adsorption in $CaBr_2$ followed the same sigmoidal trend as observed for MgI_2. The $CaBr_2$ frequency shift does have some second order components, but this is from the bandwidth shift, since the real and imaginary parts of the permittivity should be coupled in the usual way by the Kramers-Kronig relations.[26,27]

As seen from the scatting intensity of two Bragg peaks in Fig. 7 there is a phase change occurring from 1.6 h to 3.5 h. Dielectric losses have been known to vary quite dramatically with phase changes in material[28] and the features in the bandwidth shift correlate very well with change in intensities from one phase to another. From 0 to 1.6 h the bandwidth increases consistently with the increase in Bragg peak intensity (3.11 Å) related to the $Ca[NH_3]_2Br_2$ phase. From 1.6 h to 3.5 h the material is transitioning from the $Ca[NH_3]_2Br_2$ to the $Ca[NH_3]_8Br_2$ phase and the bandwidth decreases over that period. This decrease in bandwidth is believed to be due the increasing unit cell size of the material and therefore an increase in bond length of the dipolar bonds that determine dielectric loss strength. A shorter dipolar bond length relates to a stronger dielectric loss per molecule as would be the case in $Ca[NH_3]_2Br_2$ and a longer dipolar bond length relates to a weaker dielectric loss per molecule as would be the case in $Ca[NH_3]_8Br_2$ phase. After 3.5 h to sample is completely consists of

the larger $Ca[NH_3]_8Br_2$ (Bragg peak 2.96 Å) unit cell. However the material is not yet saturated and ammonia is still adsorbed into the vacant sites of the $Ca[NH_3]_8Br_2$ phase. This can be seen in the bandwidth shift from 3.5 h onwards as the bandwidth shift increases in the same fashion as the adsorption of the $Ca[NH_3]_2Br_2$ phase from 0 to 1.6 h.

In the experiment the volume increase experienced by the sample caused impeded gas flow through the quartz tube and thus leaded to sample blocking the gas flow completely. Because of this the gas flow was stopped at 4 h into the experiment due to pressure increase in the system from 1 Bar to 1.5 Bar. The sample was then left in an ammonia atmosphere and was not reflowed with argon. The pressure of the system slowly dropped by 0.2 Bar an hour, which is due to ammonia still slowly percolating through the material or escaping through leaks in the gas line.

The amount of ammonia adsorbed and ammonia per unit formula were calculated using eqn (3) and (4). The number of moles of ammonia adsorbed and ammonia per unit formula came to 0.041 and 5.45, respectively. However because the frequency shift during adsorption was not completely linear (adding error in calculation) and the sample blocked the gas flow (inability to quantify physisorbed ammonia and if the sample reached saturated ammonia adsorption) this result does not truly represent the coordination achieved throughout the whole sample.

Conclusions

We have successfully demonstrated the simultaneous microwave dielectric, neutron diffraction and mass spectroscopy characterisation of ammonia adsorption in group two halides. By following either the change in Bandwidth or frequency shift of the resonance signal we are able, by cross correlation with structural and spectroscopic measurements; determine the amount of ammonia present within the solid. Both Bandwidth and frequency shift give a measure of the total amount of ammonia within the solid, including both coordinated and physisorbed ammonia, with Bandwidth mostly affected by physisorbed ammonia.

When dielectric measurements are carried out simultaneously with mass spectroscopy and diffraction measurements, unprecedented information on the processes of ammonia adsorption may be obtained. Diffraction information provides direct information as to amount of crystallographic, metal-coordinated ammonia and, in conjunction with mass spectroscopy, can provide information on the kinetics of such processes. Furthermore, when combined with dielectric characterisation we are able to see subtleties in phase transformation processes that involve changes in dipolar bond strength in ammonia (for $CaBr_2$) and differentiation of physisorbed and metal-coordinated ammonia species (MgI_2) that are not observable by more traditional techniques. Thus, microwave dielectric characterisation is shown to be excellent probe for the ammonia content of solid state systems and may be employed – in systems that have been appropriately quantified by parallel or simultaneous structural and/or mass spectroscopy studies – as a direct measure of ammonia within a system. Furthermore, the difference in sensitivity between Bandwidth and frequency shift allows us to differentiate between metal-coordinated and physisorbed ammonia. When simultaneous, dynamic structural and dielectric measurements are employed considerable additional information that is not apparent from standard on the phase transformation mechanisms may also be elucidated.

References

1. U.S. Geological Survey, Mineral Commodity Summaries Washington, United States Government Printing Office, 2008.

2. Klerke A, Christensen C, Norskov J, Vegge T. Ammonia for hydrogen storage, challenges and opportunities, Journal of materials chemistry, 2008, 18, p. 2304-2310.

3. Leineweber A, Friedriszik M, Jacobs H, Preparation and Crystal Structures of $Mg(NH_3)_2Cl_2$, $Mg(NH_3)_2Br_2$, and $Mg(NH_3)_2I_2$, Journal of solid state chemistry, 1999, 147, p. 229-234.

4. Lepinasse E, Goetz V, Crosat G, Modelling and experimental investigation of a new type of thermochemical transformer based on the coupling of two solid-gas reactions. Chemical Engineering and Processing, 1994, 33(3), p. 125–134.

5. Elmøe T, Sørensen R, Quaade U, Christensen C, Nørskov J, Johannessen T, A high-density ammonia storage/delivery system based on $Mg(NH_3)_6Cl_2$ for – in vehicles, Chemical Engineering Science, 2006, 61(8), p. 2618-2625.

6. Liu C, Aika K, Ammonia Absorption on Alkaline Earth Halides as Ammonia Separation and Storage Procedure, Bulletin of the Chemical Society of Japan, 2004, 77(1), p. 123-131.

7. Alapati S, Johnson J, Sholl D, Predicting Reaction Equilibria for Destabilized Metal Hydride Decomposition Reactions for Reversible Hydrogen Storage, J. Phys. Chem, 2007, 111(4), p. 1584–1591.

8. Kojima Y, Investigating and Understanding Solid-State Ionic Ammine Materials. In Hydrogen Energy System Using Ammonia, CMC Publishing, 2015, p. 239.

9. Kumler WD, The Dipole Moment of Ammonia in Solution. Journal of the american chemical society, 1936, 58(6), p. 1049-1050.

10. Li S, Akyel C, Bosisio R, Precise Calculations and Measurements on the Complex Dielectric Constant of Lossy Materials Using TM_{010} Cavity Perturbation Techniques, Microwave Theory and Techniques, 1981, 29(10), p. 1041-1048.

11. Krupka J, Derzakowski K, Riddle B, A dielectric resonator for measurements of complex permittivity of low loss dielectric materials as a function of temperature, Meas. Sci. Technol, 1998, 9(10), p. 1751-1756.

12. Pozar M, Microwave engineering Chichester, Wiley & sons, 1998.

13. Waldron RA, Inst AP, Perturbation theory of resonant cavities, Institution Monograph, 1960, (373), p. 272-274.

14. Lin M, Wang Y, Afsar M, Precision measurement of complex permittivity and premeability by microwave cavity perturbation technique, Spectroscopy and material properties, 2005, 1(5), p.

62-63.

15. Hull S, Smith R, David W, Hannon A, Mayers J, Cywinski R, The Polaris powder diffractometer at ISIS, Physica B: Condensed Matter, 1992, 180-181(2), p. 1000-1002.

16. Smith R, Hull S, Armstrong A, The POLARIS Powder Diffractometer at ISIS Proceedings of the Third European Powder Diffraction Conference (EPDIC-3), Mater. Sci. Forum, 1994, p. 166-169, 251-256.

17. Weatman S, Werner P. X-Ray Investigations of Ammines of Alkaline Earth Metal Halides, I. The Structures of $CaCl_2(NH_3)_8$, $CaCl_2(NH_3)_2$ and the Decomposition Product CaClOH, Acta Chemica Scandinavica, 1981, 35, p. 467-472.

18. Westman S, Werner P, Schuler T, Raldow W, X-Ray Investigations of Ammines of Alkaline Earth Metal Halides. I. The Structures of $CaCl_2(NH_3)_8$, $CaCl_2(NH_3)_2$ and the Decomposition Product CaClOH, Acta Chemica Scandinavica, 1981, 35, p. 467-472.

19. Liu CY, Aika Ki, Effect of the Cl/Br Molar Ratio of a $CaCl_2$ - $CaBr_2$ Mixture Used as an Ammonia Storage Material, Ind. Eng. Chem. Res, 2004, 43, p. 6994-7000.

20. Jones MO, Royse DM, Edward PP, David WI, The structure and desorption properties of the ammines of the group II halides, Chemical Physics, 2013, 427, p. 38-43.

21. Hartley J, Porch A, Jones M, A non-invasive microwave method for assessing solid-state ammonia storage, Sensors & Actuators: B. Chemical, 2015, 210, p. 726-730.

22. Rubinger C, Costa L, Building a resonant cavity for the measurement of microwave dielectric permittivity of high loss materials, Microwave and Optical Technology Letters, 2007, 49(7), p. 1687-1690.

23. Bone S, Gascoyne P, Pethig R, Dielectric Properties of Hydrated Proteins at 9.9 GHz, J. Chem. Soc, 1977, 73, p. 1605-1611.

24. Davies M, Dielectric Absorption, Q. Rev. Chem. Soc, 1954, 8, p. 250-278.

25. Fish K, Miller R, Smyth C, Microwave Absorption and Molecular Structure in Liquids. XXIV. The Dielectric Relaxation of Liquid Ammonia, The Journal of Chemical Physics, 1958, 29(4), p. 745.

26. Roessler D, Kramers-Kronig analysis of reflection data, Br. J. Appl. Phys, 1965, 16, p. 1119-1123.

27. Lovell R, Application of Kramers-Kronig relations to the interpretation of dielectric data, J. Phys. C: Solid State Phys, 1974, 7, p. 4378-4384.

28. Zou C, Fothergill J, Rowe S, The effect of water absorption on the dielectric properties of epoxy nanocomposites, Dielectrics and Electrical Insulation, 2008, 15(1), p. 106 - 117.

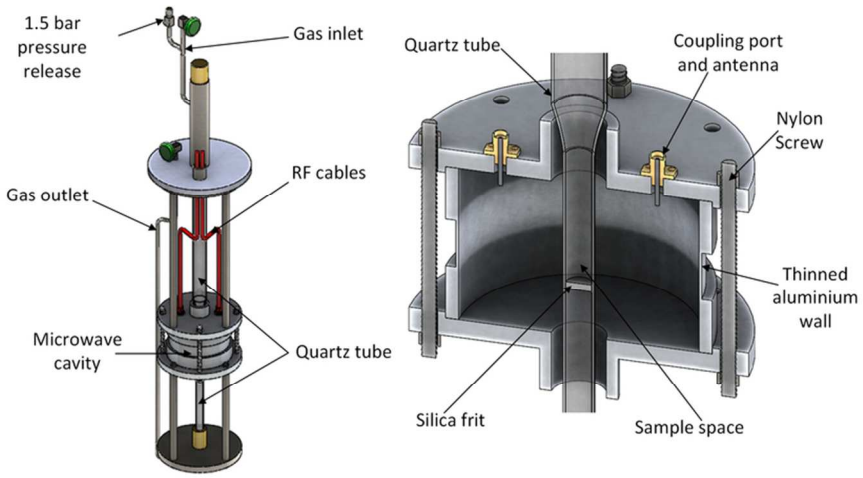

Fig. 1 - Schematic diagram of the experimental housing for the MCR in the Polaris neutron diffractometer (left) and the MCR showing internal positon of components (right).

80x38mm (300 x 300 DPI)

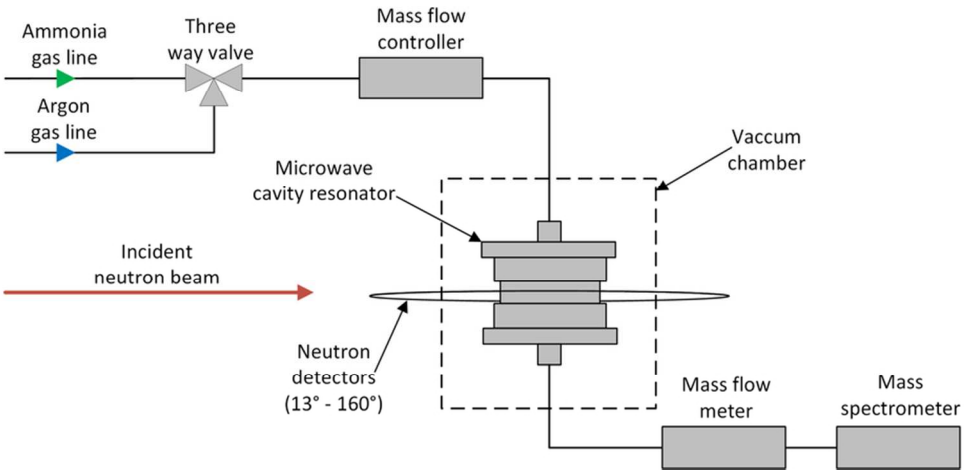

Fig. 2 - Schematic diagram of the simultaneous neutron diffraction and microwave measurement setup, showing neutron beam, gas lines and measurement apparatus.

80x38mm (300 x 300 DPI)

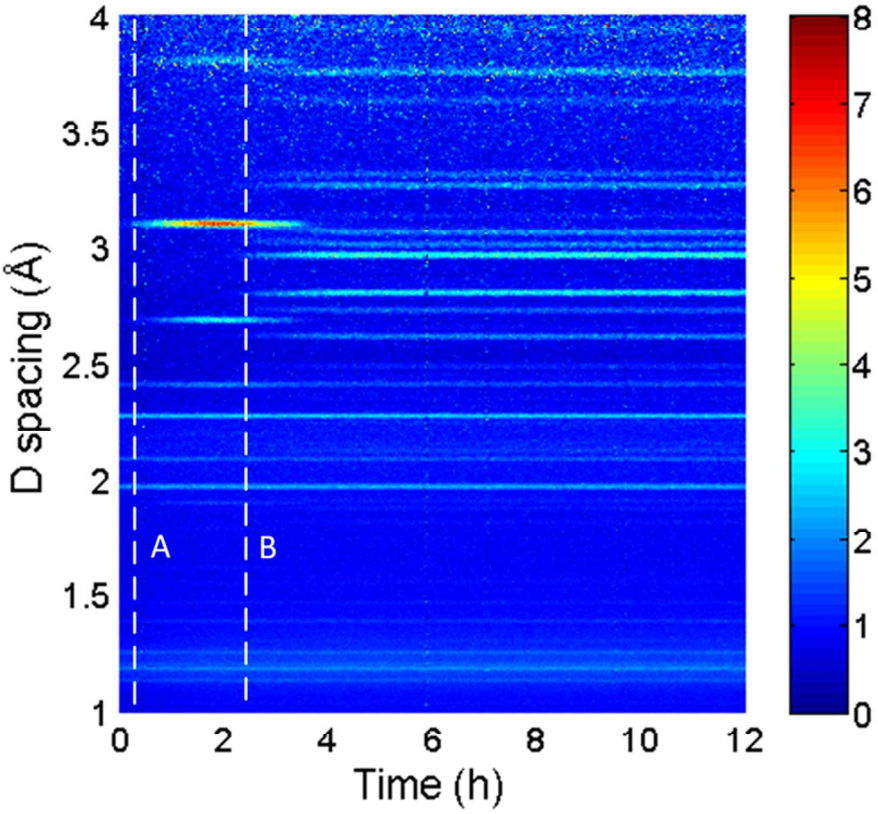

Fig. 3 - Diffraction peaks from bank 4 (90° detectors), showing neutron count in colour intensity for CaBr2 for sample weight of 1.5 g and ammonia gas flow of 5 cm3/min, where A relates to the onset of the n=2 phase and B relates to the onset of the n=8 phase.

75x67mm (300 x 300 DPI)

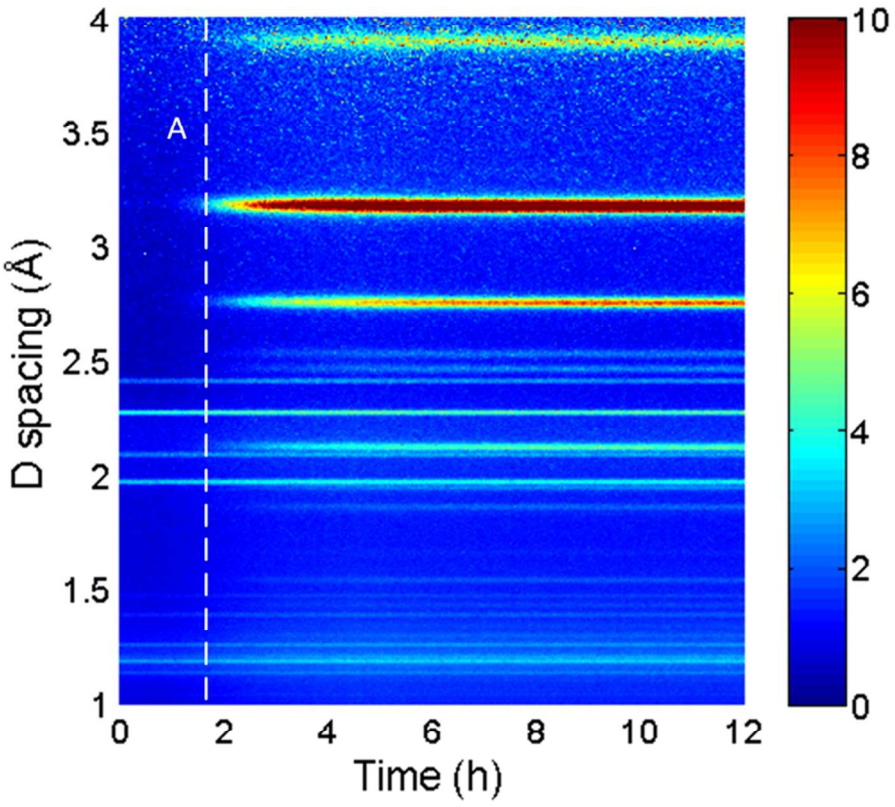

Fig. 4 - Diffraction peaks from bank 4 (90° detectors), showing neutron count in colour intensity for MgI2 for sample weight of 1.5 g and ammonia gas flow of 5 cm3/min, where A relates to the onset of the n=2 and n=6 phase.

75x67mm (300 x 300 DPI)

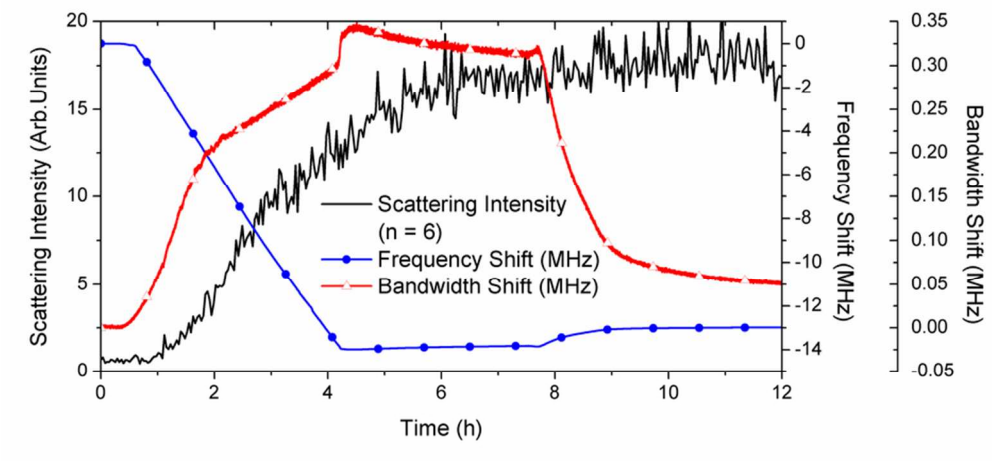

Fig. 5 - Plot of Bragg peak intensity for Mg[NH3]6I2 peak at 3.17 Å vs. frequency shift (MHz) and change in bandwidth for ammonia adsorption by MgI2. The dramatic change in dielectric properties occurs with Bragg peak intensity. It should be noted that the dielectric properties change ahead of observation by diffraction alone demonstrated the sensitivity of the dielectric technique of physisorbed and amorphous materials. The change in dielectric properties was observed to continue until the Bragg peak intensity saturated (4.2 h) at which point the shift in frequency and change in bandwidth both also saturate. Although not readily apparent in the diffraction data, the change in bandwidth suggests complex behaviour in the sample beyond a simple monotonic adsorption of ammonia and phase transformation.

79x37mm (300 x 300 DPI)

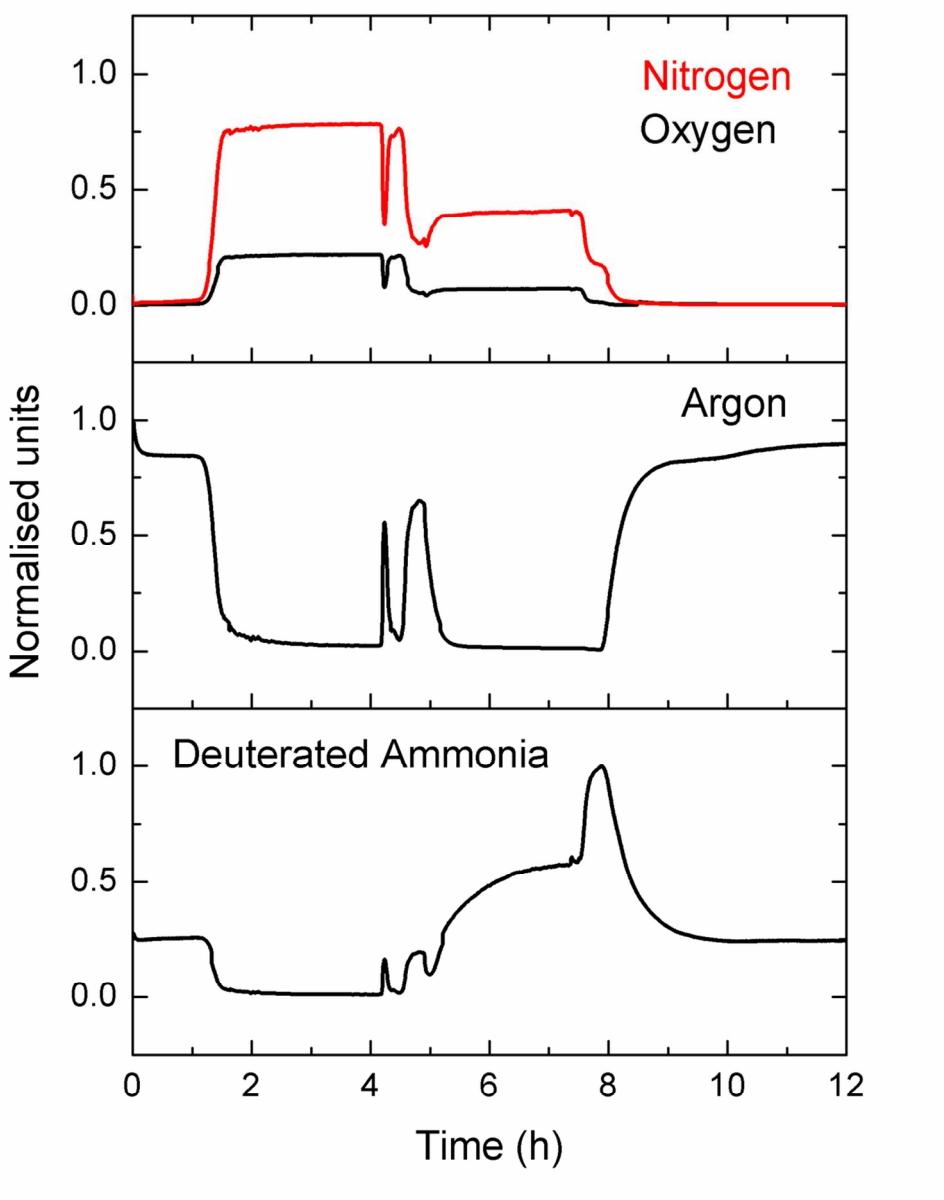

Fig. 6 - Out-gas compositions of nitrogen, argon and ammonia for ammonia adsorption of MgI2, showing increase in nitrogen content due to ammonia adsorption and the equipment aspirating air. When the gas flow is switched to argon (7.2 h) excess ammonia is observed in the out-gas.

104x132mm (300 x 300 DPI)

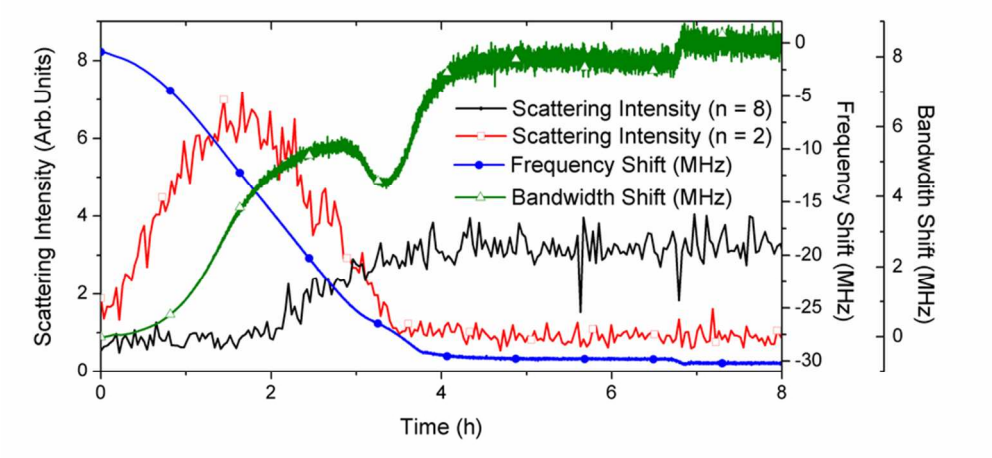

Fig. 7 - Plot of Bragg peak intensity for Ca[NH3]2Br2 (3.11 Å) and Ca[NH3]8Br2 (2.96 Å) peaks vs. frequency shift (MHz) and change in bandwidth for ammonia adsorption by CaBr2. The dramatic change in dielectric properties is shown to commence with the increase in Bragg peak intensity. This change continues to increase until the Bragg peaks saturates in intensity (1.6 h) at which point the shift in frequency and change in bandwidth both also saturate. The dip in Bandwidth and corresponding change in gradient of the Frequency shift corresponds to the change in dipolar bond length as the n=2 phase transforms into the n=8 phase.

79x37mm (300 x 300 DPI)